Mesenchymal Stromal Cells Prevent Renal Fibrosis in a Rat Model of Unilateral Ureteral Obstruction by Suppressing the Renin-Angiotensin System via HuR

Marilena Gregorini, Valeria Corradetti   , Chiara Rocca, Eleonora Francesca Pattonieri, Teresa Valsania, Samantha Milanesi, Nicoletta Serpieri, Giulia Bedino, Pasquale Esposito, Carmelo Libetta, Maria Antonietta Avanzini, Melissa Mantelli, Daniela Ingo, Sabrina Peressini, Riccardo Albertini, Antonio Dal Canton, Teresa Rampino

Abstract

We studied Mesenchymal Stromal Cells (MSC) effects in experimental Unilateral Ureteral Obstruction (UUO), a fibrogenic renal disease. Rats were divided in 5 groups: sham, UUO, MSC treated-UUO, ACEi treated-UUO, MSC+ACEi treated- UUO. Data were collected at 1, 7, 21 days. UUO induced monocyte renal infiltration, tubular cell apoptosis, tubular atrophy, interstitial fibrosis and overexpression of TGFβ, Renin mRNA (RENmRNA), increase of Renin, Angiotensin II (AII) and aldosterone serum levels. Both lisinopril (ACEi) and MSC treatment prevented monocyte infiltration, reduced tubular cell apoptosis, renal fibrosis and TGFβ expression. Combined therapy provided a further suppression of monocyte infiltration and tubular injury. Lisinopril alone caused a rebound activation of Renin-Angiotensin System (RAS), while MSC suppressed RENmRNA and Renin synthesis and induced a decrease of AII and aldosterone serum levels. Furthermore, in in-vitro and in-vivo experiments, MSC inhibit Human antigen R (HuR) trascription, an enhancer of RENmRNA stability by IL10 release. In conclusion, we demonstrate that in UUO MSC prevent fibrosis, by decreasing HuR-dependent RENmRNA stability. Our findings give a clue to understand the molecular mechanism through which MSC may prevent fibrosis in a wide and heterogeneous number of diseases that share RAS activation as common upstream pathogenic mechanism.

Abbreviations: MSC, Mesenchymal Stromal Cells; UUO, Unilateral Ureteral Obstruction; AII, Angiotensin II; RAS, Renin Angiotensin System; RENmRNA, Renin mRNA; TNFα, Tumour Necrosis Factor alfa; TGFβ, Transforming Growth Factor beta; HuR, Human Antigen R; ERK, extracellular-signal-regulated kinase; ACEi, Angiotensin Converting Enzyme inhibitor; SD, Sprague Dawley; EGFP, Enhanced Green Fluorescent Protein; P, Passage; PE, Phycoerithrin; HPF, High Power Field (x 400); FSP1, Fibroblast Specific Protein 1; TBM, Tubular Basement Membrane; MFI, Mean Fluorescence Intensity; MC, monocytes; Mϕ, macrophages

Introduction

Renal fibrosis represents the common ending of several renal diseases. Experimental Unilateral Ureteral Obstruction (UUO) has provided extensive information on renal fibrogenesis. [1–3] Different studies have shown that UUO causes a sustained glomerular ischemia, that is associated with the activation of the Renin Angiotensin System (RAS). [4–6] Angiotensin II (AII) stimulates the production of nuclear NF-kB, which recruits macrophages that release reactive oxygen species [7,8] and Tumor Necrosis Factor α (TNFα), an inducer of apoptosis and tubular atrophy. [1,9] Moreover, inflammatory cells release Transforming Growth Factor β (TGFβ) that promotes epithelial mesenchymal transition of tubular epithelial cells, while fibroblasts synthesize stress fibres and deposit extracellular matrix causing progressive interstitial fibrosis.[10–13] Furthermore, recent studies give evidence that Renin binding with its (pro)renin receptor directly prompts the extracellular-signal-regulated kinase (ERK)-dependent production of TGFβ. Therefore, Renin has a fibrogenic effect that is independent of its enzymatic action on angiotensinogen.[14–16] Human antigen R (HuR) has been recently described to stabilize RENmRNA sustaining Renin production. In the same time it has been demonstrated that HuR expression was inhibited by IL10.[17–19] Currently, RAS is the only fibrogenic system targeted by drug therapy. In fact

angiotensin-converting enzyme inhibitors (ACEi) and AII receptor blockers are used in clinic to slow down the progression of renal diseases.[20–27] MSC are isolated from several human tissues, can differentiate in multiple adult cell lineages, and display immunomodulatory properties.[28–30] When injected in animal disease models MSC migrate to sites of inflammation and injury and secrete paracrine mediators for tissue repair.[31–36] These pleiotropic activities have prompted the use of MSC for treatment of diseases where cell damage is accompanied by local and systemic inflammatory response [37–40] and for prevention of fibrosis in animal models and clinical studies.[41–44]

Here we show that MSC prevent fibrogenic kidney injury in experimental UUO and compare their effects with those of lisinopril, an ACEi. Furthermore, we report on the potential therapeutic advantage of their combined use. Finally we show that MSC suppress RAS, inhibiting HuR by IL10 release.

Materials and Methods

2.1 Animals

61 male Wild-type Sprague Dawley (SD) rats (Charles River, Lecco, Italy) weighed 250–300 g, were used for animal model. While 6 transgenic Enhaced Green Fluorescent Protein (EGFP) SD rats (Japan Slc, Hamamatsu, Japan) were used to expand MSC.[45]

Rats were housed at constant temperature (20 C°) and humidity (75%) under controlled light cycle, with free access to water and standard chow diet.

2.2 Isolation and Colture of MSC

Transgenic EGFP SD rats were sacrificed by CO_2 inhalation. Marrow cells were flushed from femurs and tibias and mononuclear cells were isolated by density gradient centrifugation (Ficoll 1077 g/ml; Lympholyte, Cedarlane Laboratories Ltd.) counted and plated in 75 or 175 cm^2 tissue culture flasks at a density of 160000/cm² in αMEM supplemented with 10% murin MesenCult (Voden, Milan, Italy) and 1% antibiotic-antimycotic (Sigma-Aldrich, Saint Louis, US). Cultures were maintained at 37°C, 5% CO_2 in a humidified atmosphere. After 48 hours, non-adherent cells were removed and culture medium was replaced twice a week. After reaching ≥80% confluence, MSC were harvested using Trypsin-EDTA (Lonza, Copenhagen, Denmark), and propagated at 4000 cells/cm².

MSC were expanded until passage (P) 4. At each passage, viable cells were counted using 0.1% eosin and culture supernatants were tested for sterility.

2.3 Immunophenotype Characterization

EGFP-MSC were characterized by flow-cytometry. Phycoerythrin (PE)-conjugated monoclonal antibodies (BD PharMingen, San Diego, US) against rat CD11b, CD45, CD90, CD49e and CD29 (Becton Dickinson, Franklin Lakes, US) using FacsCalibur flow cytometer (BD Biosciences) were used as described.[41] Appropriate, isotype-matched, non-reactive fluorochrome-conjugated antibodies were used as controls.

2.4 Differentiation assays

EGFP-MSC were evaluated for their ability to differentiate into osteoblasts and adipocytes, as previously described.[28]

The osteogenic differentiation capacity of MSC was assessed at P2-4 by incubating cells with αMEM, 10% FBS, 1% gentamicin, supplemented with 10^{-7}M dexamethasone (Sigma-Aldrich, St Louis, US), 50 mg/ml L-ascorbic acid (Sigma-Aldrich). Starting from day 7 of culture, 5 mM β-glycerol phosphate (Sigma-Aldrich) was added to the medium. Adipogenic differentiation was evaluated at P2-4 by incubating cells with αMEM, 10% FBS, 1% gentamicin supplemented with 10^{-7}M dexamethasone, 50 mg/ml L-ascorbic acid, 100 mg/ml insulin, 50 mM isobutyl methylxanthine (Sigma-Aldrich), 0.5 mM indomethacin (MP Biomedica, Illkirch, France) and 5 mM β-glycerol phosphate. Both osteogenic and adipogenic cultures were incubated for 21 days before evaluating differentiation. To detect osteogenic differentiation, cells were stained for alkaline phosphatase activity using Fast Blue (Sigma-Aldrich) and, for calcium deposition, by Alizarin Red S staining (Sigma-Aldrich). Adipogenic differentiation was evaluated through the morphological appearance of fat droplets stained with Oil Red O (Bio Optica, Milan, Italy).

2.5 *In vivo* experiments

In vivo experiments were performed according to guidelines of our ethical committee for animal studies and approved by ministerial ordinance n° 36262.

SD rats were anesthetized using intramuscular injection of Zolazepam-Tiletamine (30 mg/Kg) (Zoletil). After the induction of anesthesia a flank incision was made and the right ureter was ligated with 5/0 silk suture to induce obstruction. Animals were divided in 5 groups: Sham: 8 rats sham operated. Vehicle: 8 rats received 1 ml of saline solution after UUO at day 0 via tail vein. MSC: 8 rats received one dose of MSC ($3X10^6$) after UUO at day 0 via tail vein. ACEi: 8 rats received lisinopril in the drinking water (100 mg/L) from days 1 to 21. ACEi+MSC: 8 rats received one dose of MSC ($3X10^6$) on day 0, and ACEi from days 1 to 21. Rats were sacrificed at day 7 and 21 after ureteral ligation. Blood samples were collected at 7 and 21 days, centrifuged and maintained at -20°C until analyses were performed.

Another set of experiments was performed using 3 groups of rats sacrificed 1 day after ureteral ligation: Sham: n = 5, Vehicle: n = 8, MSC: n = 8. Soon after sacrifice kidneys were removed, half was fixed in 10% neutral-buffered formalin, half frozen in liquid nitrogen.

2.6 Biochemical measurements

Serum creatinine levels were measured by an automated method (Abbott Laboratories, Chicago, Illinois, US). Serum AII levels were quantified by ELISA (LifeSpan BioSciences, Newton, US). Serum aldosterone levels were measured by chemiluminiscent assay (Liaison Aldosterone assay, DiaSorin, Vercelli, Italy).

For dosage of Renin and TGFβ in renal tissue the kidneys were homogenized in 0.1 M tris HCL, pH 7.4, containing 8-hydroxyquinolone sulfate (3.4mM), 0.25 EDTA, 0.1 phenylmethysulfonyl fluotide, 1,6 dimercaprol, 5 sodium tetrathionate, and 0.1% Triton X-100. The concentration of proteins was determined with a bicinchoninic acid protein assay kit (Pierce, Rockford, IL, US). After centrifugation of the homogenate, supernatant was collected and stored at -70°C. Renin levels were measured in renal tissue at day 7 by chemiluminiscent assay (DiaSorin), using monoclonal antibody (mouse) that recognizes Renin and prorenin. TGFβ levels were measured in renal tissue by Quantikine ELISA Kit (R&D Systems, Minneapolis, US), that recognizes rat TGFβ in surnatant.

2.7 RNA Extraction and Real time PCR

Total RNA was extracted from renal tissue and cultured cells (HK2 cell line and macrophages) using respectively trizol method and guanidine based RNeasy® Mini Kit (QIAGEN Venlo, Holland). RNA was treated with DNase from RNase-Free DNase Set (QIAGEN) and dissolved in nuclease free water. Extracted RNA was tested for quantity and integrity by spectrophotometric analysis (NanoDrop, Thermo Scientific, Watham, US). A total of 1 µg of RNA per condition was reverse transcribed into cDNA through 1st Strand cDNA Synthesis Kit for RT-PCR (AMV) (Roche Applied Science, Basel, Germany). cDNA was used to perform real-time PCR analysis in 96-well optical reaction plates, using ABI prism 5700 (Applied Biosystems, Watham, US) and the 5-exonuclease assay (TaqMan technology) in a volume of 25 µl reaction containing Taqman Universal Master Mix, optimized concentrations of FAM-labeled probe, and specific forward and reverse primers for βactin, Renin and HuR (Applied Biosystems, Watham, US; catalogue number Rn00667869_m1, Rn00561847_m1 and Rn01403240_m1, respectively). Water replacing cDNA was included in real-time PCR as controls. The results were analyzed using a comparative method, and values normalized to the βactin expression and converted into fold change.

2.8 Renal Histopathology

2.8.1 Apoptotic nuclei.

Renal sections were dewaxed in xylol, passed in a decreasing series of alcohol, and finally rehydrated with distilled water. For permeabilization the tissues sections were exposed to distilled water containing 0.1%Triton X-100, 0.1% citrate sodium, then incubated with proteinase K in Tris/HCl10mM, pH 7.4–7.8. After washing in PBS, sections were incubated with 20 ml of TUNEL reaction mixture (In Situ Cell Death Detection Kit, Fluorescein, Roche) for 1 hour at 37°C, in a dark humid chamber. After washing in PBS, specimens were mounted in Vectashield Mounting Medium with DAPI (Vector Laboratories, Burlingame, US) and examined with fluorescence microscope Nikon E400 with CCD camera and software imaging analysis Cell-R. In order to assess apoptotic nuclei we examined 10 non-overlapping fields per renal section (X400) per animal and expressed them as means ± SD.

2.8.2 Renal Morphology.

3 µm thick sections of formalin-fixed kidney were examined by two investigators in double blind fashion, using an Olympus IX8 microscope connected with a CCD camera and software imaging analysis Cell-R.

Tubule diameters were analyzed in 10 non consecutive fields (X400) per kidney section. Results were expressed as µm (means ± SD). The percentage of broken tubules/High Power Field (HPF) was evaluated in 10 non consecutive fields (X400) per renal section. Results were expressed as percentage of broken tubules/HPF. Interstitial fibrosis was measured by Masson's trichrome staining (score 1–4): 1: Masson's trichrome positive area/HPF <25%, 2: Masson's trichrome staining involving 26 to 50%, 3: Masson's trichrome staining involving 51 to 75%, 4: Masson's trichrome staining involving >75%. The results were expressed as means ± SD.

2.8.3 EGFP, ED1 Ag and Fibroblast Specific Protein 1 (FSP1) expression.

EGFP, ED1 Ag and FSP1 renal expression were studied by immunohistochemistry (IHC) in formalin fixed tissue. Three-µm thick sections of paraffin embedded tissue were collected on poly-L-lysine-coated slides (Dako, Glostrup, Denmark), they were dewaxed in xylol, passed in a decreasing series of alcohol, and finally rehydrated with distilled water. Endogenous peroxidase was blocked with H_2O_2/methanol 3.7% vol/vol for 10 minutes followed by H_2O. After 3 washings in PBS sections underwent microwave antigen retrieval, then were exposed overnight at 4°C to the following antibodies: 1) monoclonal mouse anti-green fluorescent protein antibody IgG1 (Chemicon International, Billerica, US), 2) monoclonal mouse anti-rat ED1 (Serotec Ltd, Kidlington, UK), 3) polyclonal anti S100-A4 (Dako). After 3 washings in PBS the immunocomplex was visualized with the biotin-streptavidin-peroxidase complex and 3,3-diaminobenzidine (Dako). Sections were faintly counterstained with Harris hematoxylin. Negative controls included both omission of the primary Ab and substitution of IgG for primary antibodies. The positive controls for EGFP were kidney sections of SD-EGFP. In 10 renal sections per kidney we counted EGFP, ED1 and FSP1 positive cells/HPF. Since EGFP cells were spontaneously fluorescent we studied EGFP renal expression also by fluorescence method. Renal sections were air dried and post-fixed in ethanol 70%, 95%, 100% (3 min). After washing in PBS, specimens were mounted in Mowiol Mounting Medium (Sigma-Aldrich) and examined with fluorescence microscope Nikon E400 with CCD camera and software imaging analysis Cell-R.

2.9 In vitro experiments

HK2 cell line (ATCC® CRL-2190™, Manassas, US) was used to assess Renin production in co-culture experiments. Cells were planted in 6-well plates at concentration of 1×10^6/well in Low Glucose (LG) Medium: RPMI 1640, 10% Fetal Calf Serum (FCS) (EuroClone, Pero, Italy), 1% insulin-transferrin-selenium and 1% penicillin/strepromycin (Gibco, Waltham, UK), and incubated at 37°C, 5% CO_2. High Glucose (HG) medium was prepared adding 6 g/L (30mM) of glucose to LG medium. MSC/HK2 were planted in well at ratio of 1:2, 1:20 and 1:200 in LG medium. After 24h, medium was replaced with HG-medium for 4h then cells were collected for RNA extraction.

In additional experiments, HK2 were cultured in HG: a) additioned with IL10 (10 ng/ml) (R&D Systems) for 1h, b) co-cultured with MSC (1:2) and anti IL10 blocking antibody (100 ng/ml) (Pierce-Endogen, Rockford, US) for 4h. Cells were collected for RNA extraction.

Monocytes (MC) were isolated from heparinized blood by density gradient centrifugation (Lymphoprep, Stemcell Technologies, Vancouver, Canada), and plated at $1x10^6$/well in RPMI1640 supplemented with 10% human AB positive serum, 1% penicillin/streptomycin to induce macrophage (Mφ) differentiation. After 24h of adherence cells were scraped. Mφ differentiation was confirmed by flow cytometer analysis using anti CD14, anti CD11b, anti CD31 and anti CD62L (BD Pharmingen). Mφ were than cultured with MSC at different ratios (MSC/Mφ 1:2, 1:20 and 1:200) for 4 days at 37°C, 5% CO_2.

In additional experiments, Mφ were cultured: a) with IL10 (10 ng/ml) (R&D Systems) for 4h, b) co-cultured with MSC (1:2) and anti IL10 blocking antibody (100 ng/ml) (Pierce-Endogen) for 24h. Cells were collected for RNA extraction.

2.10 Statistical analysis

ANOVA followed by the Newman-Keuls test were used to compare not parametric variables and Student t test for the means.

Results

3.1 Rat MSC characterization

EGFP-MSC showed the typical spindle shape morphology (Fig 1, panel 1) and resulted positive for CD49, CD90, and CD29, while they were negative for CD45 and CD11b. (Fig 1, panel 2) MSC exhibited the capacity to differentiate *in vitro* to osteoblasts and adipocytes as confirmed by histological staining. Microscopic examination of stained cells demonstrated the presence of mineralization nodules and fat droplets. (Fig 1, panel 3)
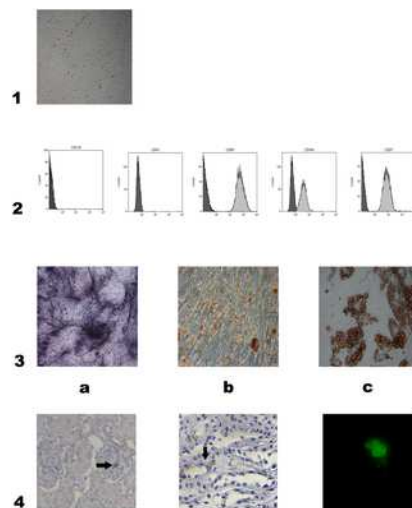

Fig 1. Characterization and localization of rat EGFP-MSC.
1: Characteristic spindle-shaped morphology of bone marrow derived MSC obtained from one rat. Magnification X4. 2: Immunophenotype of one representative culture-expanded rat EGFP-MSC. Rat MSC were negative for CD11b and CD45 and positive for CD90, CD49e and CD29. 3: Osteogenic and adipogenic differentiation capacity of rat MSC. Differentiation into osteoblasts was demonstrated by the histological detection of Alkaline phosphatase activity (a) and calcium depositions positive for Alizarin Red (b). Differentiation into adipocytes was revealed by the formation of lipid droplets stained with Oil Red O (c). Magnification X20. 4: Representative renal sections of rats treated with MSC sacrified one day after ureteral ligation. Arrows indicate EGFP positive MSC. Immunohistochemistry for EGFP showing glomerular (a) tubular and interstitial (b) localization of MSC, magnification X200. Self fluorescence showed EGFP-MSC presence (c), magnification X400.
https://doi.org/10.1371/journal.pone.0148542.g001

3.2 *In vivo* experiments

Through the study period, no significant differences were observed in body weight, water and food intake among the 5 groups of rats. No side effects were documented.

3.3 MSC localization

In EGFP-MSC treated rats, few cells were tracked (0–5 per section/HPF), on kidney sections obtained at day 1, and they were located in glomeruli, tubules and interstitium. (Fig 1, panel 4)

3.4 Renal function

At 7 and 21 days serum creatinine levels were significantly higher in UUO compared to sham (p<0.05). There was no difference

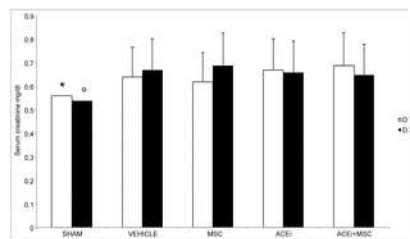among groups of obstructed rats, nor between day 7 and day 21 (Fig 2)

Fig 2. Serum creatinine levels at 7 and 21 days after UUO in sham, vehicle, MSC, ACEi, ACEi+MSC groups.
D7 and D21 indicate the day after UUO, columns represent serum creatinine levels, bars represent SD. Data are mean ± SD.
*p<0.05 vs all groups, °p<0.05 vs all groups.
https://doi.org/10.1371/journal.pone.0148542.g002

3.5 RENmRNA expression, Renin tissue levels, AII and aldosterone serum levels

After 7 days of UUO, RENmRNA expression significantly increased in renal tissue of all groups except for MSC D7 (p<0.001), while in MSC and ACEi+MSC groups RENmRNA expression decreased in comparison to vehicle and ACEi groups (p<0.05), suggesting a MSC inhibitory effect on RENmRNA expression. (Fig 3, panel A)
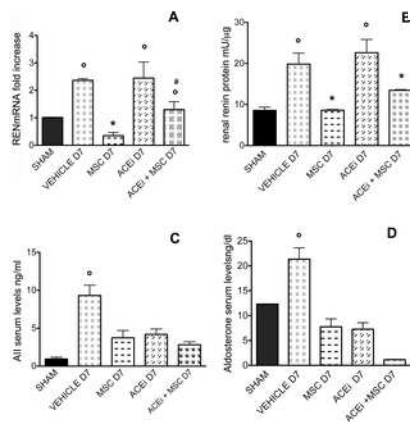

Fig 3. REN mRNA, renal Renin, serum AII and aldosterone levels.
D7 indicates the day after ureteral ligation. A: RENmRNA expression in all groups of rats determined by real time PCR. Columns indicate RENmRNA expression normalized to the βactin expression and converted in fold change. °p<0.001 vs sham, *p<0.05 vs vehicle D7, ACEi D7 and ACEi+MSC D7, #p<0.05 vs ACEi D7. B: Renin protein levels in renal tissue in all groups of rats. Columns represent Renin protein levels. Data are means ± SD. °p<0.005 vs sham, MSC D7 and ACEi+MSC D7, *p<0.05 vs vehicle D7 and ACEiD7. C: AII serum levels in all groups of rats. Columns represent AII levels. Data are means ± SD. °p<0.005 vs all groups. D: Aldosterone serum levels in all groups of rats. Columns represent aldosterone serum levels. Data are means ± SD. °p<0.005 vs all groups.
https://doi.org/10.1371/journal.pone.0148542.g003

Accordingly, at day 7 Renin tissue levels increased in vehicle and ACEi rats compared to sham, while in MSC and ACEi+MSC groups they were significantly decreased compared to vehicle and ACEi rats (p<0.05). (Fig 3, panel B)

As sign of RAS activation, after 7 days AII and aldosterone serum levels significantly increased in UUO rats (p<0.005). MSC, ACEi and combined therapy induced a significant decrease in AII and aldosterone serum levels (p<0.005). (Fig 3 panels C and D, respectively)

3.6 Monocyte infiltrate

As shown in Fig 4 panel B, UUO induced a significant MC infiltration increase in renal tissue (p<0.0001). After 7 days of ligation, MC were significantly reduced by MSC and ACEi+MSC (p<0.001). Moreover combined therapy significantly reduced MC infiltration compared to ACEi (p<0.05). At 21 day, MC infiltration was significantly reduced by all treatments (p<0.0001). (Fig 4, panel B)
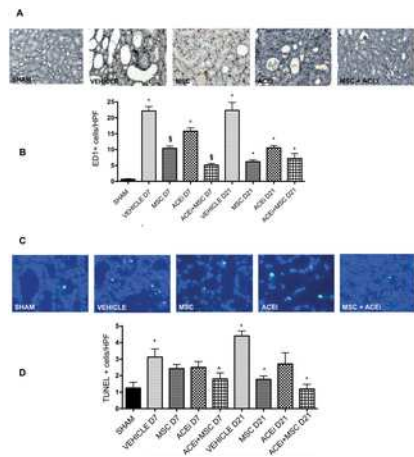
Fig 4. Monocyte infiltrate and tubular apoptosis.
A: *Monocyte infiltrate.* Representative renal sections of all groups of rats sacrified 7 days after ureteral ligation stained for ED1 binding cells. Magnification, X200. B: Columns represent ED1 binding cells/HPF (means ± SD). Kidneys studied at day 7 and day 21. °p<0.0001 vs sham, §p<0.0001 vs vehicle D7, ^p<0.05 vs MSC D7 and ACEi+MSC D7, *p<0.0001 vs vehicle D21. C: *Tubular apoptosis.* Representative renal sections of all groups of rats sacrified 21 days after ureteral ligation stained with DAPI to evaluate apoptotic nuclei. Magnification, X400. D: Columns represent apoptotic nuclei/HPF (means ± SD). Kidneys studied at day 7 and day 21. *p<0.05 vs Sham, ^p<0.05 vs Vehicle D7, °p<0.005 vs Vehicle D21.
https://doi.org/10.1371/journal.pone.0148542.g004

3.7 Apoptosis

Tunel tubular positive cells increased significantly after 7 and 21 days of ureteral ligation in vehicle rats compared to sham operated rats (p<0.005). At day 7, ACEi+MSC treatment significantly decreased tubular cell apoptosis (p<0.05). At day 21 MSC and ACEi+MSC treatment significantly decreased tubular cell apoptosis (p<0.005). (Fig 4, panel D)

3.8 Tubular damage

Tubular damage was evaluated at day 7 by measuring tubular diameters and at day 21 by enumerating damaged Tubular Basement Membrane (TBM). Tubular diameter was significantly increased in UUO compared to sham (p<0.0001). Renal sections of MSC, ACEi and ACEi+MSC treated rats showed tubules with significantly smaller diameters compared to vehicle (p<0.05). (Fig 5, panel B)
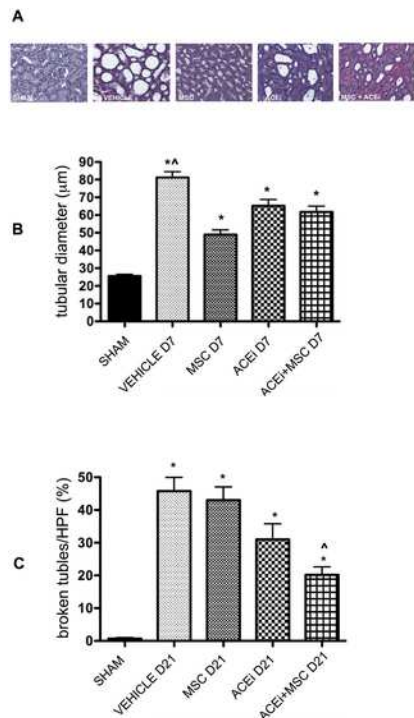
Fig 5. Tubular damage.
A: *Tubular diameters*: Hematoxylin-eosin staining of representative renal sections of all groups of rats at day 7. Magnification, X200. B: *Tubular diameters* columns represent tubule diameters/HPF at day 7, results expressed as means ± SD. *p<0.0001 vs sham, ^p<0.05 vs MSC D7, ACEi D7 and ACEi+MSC D7. C: *Broken tubules*. Columns represent percentage of broken tubules/HPF at day 21. Results were expressed as means ± SD. *p<0.0001 vs sham, ^p<0.01 vs MSC D21 and Vehicle D21.
https://doi.org/10.1371/journal.pone.0148542.g005

The number of tubules with damaged TBM was significantly reduced by combined therapy compared to vehicle and MSC alone (p<0.01). (Fig 5, panel C)

3.9 Renal tissue TGFβlevels

After 7 days of UUO, tissue TGFβ levels increased in vehicle group. In all treated groups, TGFβ levels were significantly lower (p<0.05). (Fig 6, panel B)
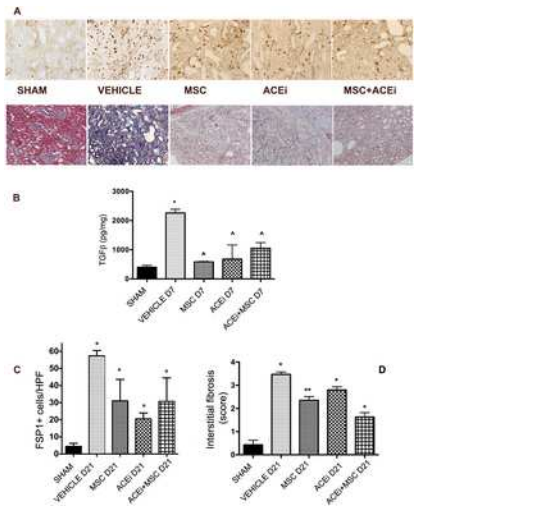

Fig 6. Renal fibrosis.
A: Upper: Representative renal sections of IHC for FSP1 in all groups at day 7 (X200). Bottom: Representative renal sections of Masson's trichrome staining in all groups at day 21 (X200). B: *Renal tissue TGF*β *levels*. Columns represent tissue TGFβ levels after 7 days from ureteral obstruction in all groups. Data are means ± SD. *p<0.001 vs sham, ^p<0.05 vs Vehicle D7. C: *FSP1 positive cells*. Columns represent FSP1 positive cells/HPF (means ± SD) at day 21. *p<0.001 vs all groups, °p<0.005 vs vehicle D21. D: *Interstitial fibrosis score* Columns represents the score of interstitial fibrosis (means ± SD) at day 21. *p<0.05 vs sham, °p<0.001 vs vehicle D21.
https://doi.org/10.1371/journal.pone.0148542.g006

3.10 Renal fibrosis

Fibrosis was defined both as FSP1 positive cells/HPF and Masson's trichrome positive area/HPF (X400). After 21 days of obstruction FSP1 positive cells increased significantly in non treated animals (p<0.001). (Fig 6, panel C) A significant decrease of fibroblast amount was observed following ACEi, MSC and combination therapies (p<0.005). Masson's trichrome staining showed that fibrosis score was significantly (p<0.001) less severe in rats treated both with MSC and ACEi+MSC compared to untreated rats at day 21. (Fig 6, panel D)

3.11 Renal Human antigen R (HuR) mRNA, RENmRNA expression and Renin levels at day 1

HuRmRNA, RENmRNA expression and Renin levels increased significantly 1 day after ureteral ligation in non treated animals (p<0.001). MSC treatment inhibited HuRmRNA, RENmRNA expression and Renin levels. (Fig 7)

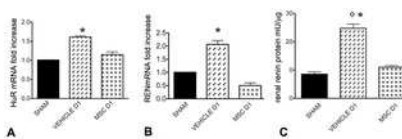**Fig 7. HuRmRNA, RENmRNA expression and renal Renin levels.**
A: HuRmRNA expression in Sham, Vehicle and MSC groups one day after ureteral ligation determined by real time PCR. Columns indicate HuRmRNA expression normalized to the βactin expression and converted in fold change. *p<0.001 vs Sham and MSC D1. B: RENmRNA expression in Sham, Vehicle, and MSC groups one day after ureteral ligation determined

by real time PCR. Columns indicate RENmRNA expression normalized to the βactin expression and converted in fold change. *p<0.001 vs Sham, MSC D1. C: Renal Renin levels in Sham, Vehicle and MSC groups one day after ureteral ligation. Columns represent Renin levels. Data are means ± SD. °p<0.005 vs MSC D1, *p<0.0001 vs sham.
https://doi.org/10.1371/journal.pone.0148542.g007

3.12 *In vitro* experiments

3.12.1 MSC/HK2 co-coltures.

RENmRNA expression, as expected, was significantly higher in HK2 cultured in high glucose (HG) medium than in low glucose (LG) medium (p<0.05). (Fig 8, panel A) Presence of MSC in HK2 HG cultures reduced RENmRNA expression in a dose dependent manner. At 1:2 MSC/HK2 ratio RENmRNA expression was similar to HK2 LG expression. (Fig 8, panel A)
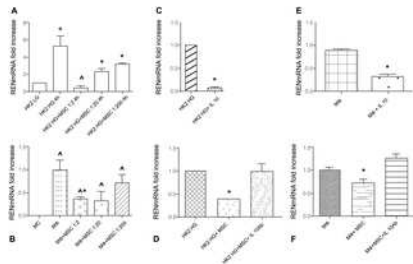

Fig 8. RENmRNA expression in co-coltures of MSC and HK2 or Mφ.
A: RENmRNA expression in HK2 cultured in low glucose (LG) medium, high glucose (HG) medium, in co-coltures with MSC (1:2, 1:20, 1:200) for 4 h. Columns indicate RENmRNA expression normalized to the βactin expression and converted in fold change. °p<0.05 vs HK2 LG; HK2 HG + MSC 1:2 4h. ^p< 0.01 vs HK2 HG + MSC 1:20 4h, HK2 HG + MSC 1:200 4h. *p<0.01 vs HK2 LG. B: RENmRNA expression in circulating monocytes (MC), macrophages (Mφ), MSC+Mφ co-coltures (1:2, 1:20, 1:200) for 4 days. Columns indicate RENmRNA expression normalized to βactin expression and converted in fold change. ^p<0.01 vs MC, *p<0.005 vs Mφ. C: RENmRNA expression in HK2 cultured in HG medium in presence and absence of IL10 (10 ng/ml) for 1 h. *p<0.001 vs HK2 HG. D: RENmRNA expression in HK2 cultured in HG medium, in MSC/HK2 HG co-coltures (1:2) in presence and absence of anti IL10 blocking antibody at concentration 100 ng/ml for 4 h. Columns indicate RENmRNA expression normalized to the βactin expression and converted in fold change. *p<0.0001 vs HK2 HG, HK2 HG+MSC+anti IL10 Ab. E: RENmRNA expression in Mφ cultured in presence and absence of IL10 (10 ng/ml) for 4 h. Columns indicate REN mRNA expression normalized to βactin expression and converted in fold change. *p<0.05 vs Mφ. F: RENmRNA expression in Mφ, MSC/Mφ co-coltures (1:2) in presence and absence of anti IL10 blocking antibody at concentration 100 ng/ml for 24 h. Columns indicate RENmRNA expression normalized to βactin expression and converted in fold change. *p<0.05 vs Mφ and Mφ+MSC+IL10 Ab.
https://doi.org/10.1371/journal.pone.0148542.g008

3.12.2 MSC/Macrophages co-coltures.

Macrophage characterization after 24 h adhesion is shown in Fig 9. After 4 days MSC/Macrophages co-colture, flow cytometry analysis revealed a significant increase of cell surface CD14 expression: Mean Fluorescence Intensity (MFI) before adhesion 46, MFI post adhesion 108. RENmRNA expression in Mφ was significantly higher than in circulating MC (p<0.01).
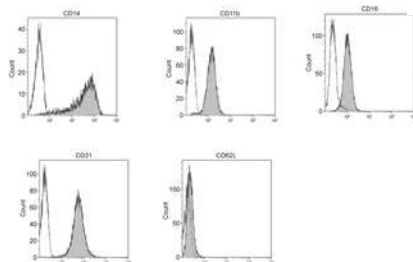
Fig 9. Representative flow cytometry analysis of monocyte-derived macrophages.
Macrophages were obtained after 24 hours of adhesion. White peaks represent negative control by isotype-matched, non-reactive fluorochrome-conjugated antibodies. Grey peaks represent positive cells.
https://doi.org/10.1371/journal.pone.0148542.g009

MSC in co-colture reduced RENmRNA expression in Mφ, significantly at 1:2 ratio (p<0.005). (Fig 8, panel B)

3.12.3 MSC modulate RENmRNA expression via IL10.

In order to investigate the mechanism through which MSC suppress RENmRNA expression, we performed *in vitro* culture experiments in presence of IL10 and anti-IL10 blocking antibody. Addition of IL10 to HK2 HG cultures significantly decreased RENmRNA expression (p<0.001). (Fig 8, panel C) While addition of anti-IL10 blocking antibody in MSC/HK2 HG co-culture reversed MSC suppression on RENmRNA expression. (Fig 8, panel D) Similarly RENmRNA expression in Mφ cultures additioned with IL10 was significantly lower than in Mφ without IL10 (p<0.05). (Fig 8, panel E) The addition of anti IL10 blocking antibody in co-cultures MSC/Mφ reversed MSC suppressive effect. (Fig 8, panel F)

Discussion

It is well documented that acute UUO is followed by a prompt renal vasodilatation that turns into a persistent vasoconstriction whithin 24 hours.[4–6] The ensuing ischemia is associated with the progressive development of tubular atrophy and interstitial fibrosis that are a proved effect of increased AII release resulting from enhanced Renin production.[2,3] In addition, recent studies have shown that Renin has a fibrogenic effect that is independent of its enzymatic release of AII. In fact, the interaction of Renin with its receptor activates the production of TGFβ transduced by the ERK system. [14–16] MSC have been shown to have an antiiflammatory and antifibrogenic effect in several models of injury to various tissues, including the kidney.[35–37,46] In the present study we have investigated whether MSC prevent UUO induced fibrosis and we have tested whether MSC operate this effect through Renin. Furthermore, we have compared the results obtained following MSC infusion with those of ACEi treatment and the combination of both in order to add therapeutic advantage. Our results show that MSC decrease tubular cell apoptosis and infiltrating monocyte number and preserve tubular integrity preventing luminal dilatation and disruption of the basement membrane. These effects were associated with a significant decrease of fibrotic renal tissue, that did not result in a significant effect on renal function, as indicated by serum creatinine levels. These findings may be argued as contradictory, but a sound explanation is provided by simply considering that the loss of renal function associated with fibrosis in the obstructed kidney is compensated by increased GFR of the contralateral organ.[47] Of course, prevention of fibrosis as operated by MSC or ACEi treatment limits the loss of function in the obstructed kidney, but does not induce any compensatory increase in controlateral function.

Kidney protection afforded by MSC was comparable to that provided by ACEi, while a further decrease of renal inflammation and interstitial fibrosis was observed with the combined use of MSC and ACEi. Our results provide more informations on the MSC therapeutic potential described in previous studies, where it has been shown that MSC injected into obstructed kidney reduce the expression of collagen synthesis, fibroblast activation [42] and infiltrating macrophage number.[37–41,43,48,49] However the main innovation of our study was to shed some light on the possible mechanism(s) that account for MSC effects. It is well known that in acute and chronic models, MSC may act by paracrine action rather than a transdifferentiation into renal resident cells. This hypothesis is supported by our finding that very few EGFP-MSC were tracked in the kidney.

Moreover, we observed that after UUO, MSC inhibited expression of RENmRNA, Renin, AII and aldosterone, suggesting that MSC may antagonize RAS. It has been shown that RAS activation induces recruitment of inflammatory cells in several disease models including UUO [7,8], with release of inflammatory, pro-apoptotic and fibrogenic cytokines that enhance tissue damage.[10,50–53] Therefore, RAS inhibition observed in MSC treated rats may also explain prevention of macrophage infiltration.

We also found that MSC abated TGFβ that plays a crucial role in generating fibrosis, because it stimulates matrix proteins synthesis, decreases matrix degradation, stimulates fibroblast proliferation and synthesis of stress fibres, promotes epithelial–mesenchymal transition of tubular cells.[11–13] This finding may be a consequence of Renin inhibition by MSC. A question raised by our study is how MSC affect Renin release. In renal tissue, granular cells of afferent arteriole are the main source of Renin, but RENmRNA is expressed in tubular cells [54,55] and infiltrating macrophages [56], too.

Since MSC prevent macrophage infiltration [44,48,49], it is reasonable to assume that one mechanism by which MSC inhibited RAS was by blocking the source of Renin represented by macrophages.[57] However, the behaviour of RENmRNA expression in rats treated with ACEi and MSC suggests that MSC directly downregulated Renin production by renal cells. We have shown that the increase in RENmRNA and Renin that occurs in ACEi treated rats is suppressed by MSC. This suppression takes place while the inhibition of AII caused by ACEi persists, so that MSC suppress Renin by a mechanism that does not involve the AII-evoked feedback. The evidence that MSC and ACEi operate RAS inhibition in a different way provides a rationale for using them in combined therapy. Actually in our study their combination strength their anti-fibrogenic effect.

In order to understand MSC mechanism, we focused on: a) Renin release, first step of RAS activation, b) HuR expression, that sustains Renin production, stabilizing RENmRNA [17–19,58,59] c) IL10, cytokine known to be produced by MSC [54–56,60,61] and able to inhibit HuR expression.[17–19]

For the first time we proved in *ex vivo* experiments that MSC reduce REN and HuR mRNA expression in obstructed kidney, already one day after UUO. To understand whether MSC inhibited REN and HuR mRNA expression via IL10, we performed *in vitro* experiments and demonstrated that MSC downregulated RENmRNA in tubular cells [62,63] and in macrophages[57]. IL10 inhibited RENmRNA expression in activated tubular cells and macrophages and the addition of anti IL10 blocking antibody in co-cultures of MSC/tubular cells and MSC/macrophages reversed MSC effects. We also measured IL10 in MSC culture surnatants but we found only slightly detectable levels (data not shown), perhaps due to the fast use of IL10 by the cells.

In conclusion, we have shown that MSC injection in UUO prevents inflammation, tubular cell apoptosis and fibrosis. These effects are associated with the suppression of RAS, macrophage infiltration and TGFβ expression. These findings allow to reconstruct a rational sequence of events that may represent a RAS inhibitory pathway driven by MSC. We confirm that RAS inhibition is associated with HuR suppression, and give evidence that MSC suppress HuR and thus inhibit RAS. IL10 released by MSC may be responsible for HuR suppression.

The present study is a further demonstration that MSC mitigate injury and/or favour repair by delivering soluble factors that in a paracrine or even endocrine manner modify the cell behaviour favouring kidney recovery.

Acknowledgments

Author Contributions

Conceived and designed the experiments: MG ADC TR. Performed the experiments: VC CR EFP TV SM NS GB PE MAA MM DI. Analyzed the data: MG TR ADC CL PE. Contributed reagents/materials/analysis tools: MAA SP RA. Wrote the paper: MG ADC TR.

References

1. Chevalier RL, Forbes MS, Thornhill BA. Ureteral obstruction as a model of renal interstitial fibrosis and obstructive nephropathy. Kidney Int. 2009;75: 1145–52. pmid:19340094
   View Article   • PubMed/NCBI   • Google Scholar

2. Klahr S, Morrissey J. Obstructive nephropathy and renal fibrosis. Am J Physiol Renal Physiol. 2002;283: F861–75. pmid:12372761
   View Article   • PubMed/NCBI   • Google Scholar

3. Truong LD, Gaber L, Eknoyan G. Obstructive uropathy. Contrib Nephrol. Karger Publishers; 2011;169: 311–26.
   View Article   • Google Scholar

4. Dal Canton A, Stanziale R, Corradi A, Andreucci VE, Migone L. Effects of acute ureteral obstruction on glomerular hemodynamics in rat kidney. Kidney Int. 1977;12: 403–11. Available: http://www.ncbi.nlm.nih.gov/pubmed/609190 pmid:609190
   View Article   • PubMed/NCBI   • Google Scholar

5. Dal Canton A, Corradi A, Stanziale R, Maruccio G, Migone L. Effects of 24-hour unilateral ureteral obstruction on glomerular hemodynamics in rat kidney. Kidney Int. 1979;15: 457–62. Available: http://www.ncbi.nlm.nih.gov/pubmed/480781 pmid:480781
   View Article   • PubMed/NCBI   • Google Scholar

6. Dal Canton A, Corradi A, Stanziale R, Maruccio G, Migone L. Glomerular hemodynamics before and after release of 24-hour bilateral ureteral obstruction. Kidney Int. 1980;17: 491–6. Available: http://www.ncbi.nlm.nih.gov/pubmed/7392422 pmid:7392422
   View Article   • PubMed/NCBI   • Google Scholar

7. Esteban V, Lorenzo O, Rupérez M, Suzuki Y, Mezzano S, Blanco J, et al. Angiotensin II, via AT1 and AT2 receptors and NF-kappaB pathway, regulates the inflammatory response in unilateral ureteral obstruction. J Am Soc Nephrol. 2004;15: 1514–29. Available: http://www.ncbi.nlm.nih.gov/pubmed/15153562 pmid:15153562
   View Article   • PubMed/NCBI   • Google Scholar

8. Sugiyama H, Kobayashi M, Wang D- H, Sunami R, Maeshima Y, Yamasaki Y, et al. Telmisartan inhibits both oxidative stress and renal fibrosis after unilateral ureteral obstruction in acatalasemic mice. Nephrol Dial Transplant. 2005;20: 2670–80. pmid:16141465
   View Article   • PubMed/NCBI   • Google Scholar

9. Docherty NG, O'Sullivan OE, Healy DA, Fitzpatrick JM, Watson RWG. Evidence that inhibition of tubular cell apoptosis protects against renal damage and development of fibrosis following ureteric obstruction. Am J Physiol Renal Physiol. 2006;290: F4–13. pmid:16339963
   View Article   • PubMed/NCBI   • Google Scholar

10. Grande MT, Pérez-Barriocanal F, López-Novoa JM. Role of inflammation in túbulo-interstitial damage associated to obstructive nephropathy. J Inflamm (Lond). 2010;7: 19.
    View Article   • Google Scholar

11. López-Hernández FJ, López-Novoa JM. Role of TGF-β in chronic kidney disease: an integration of tubular, glomerular and vascular effects. Cell Tissue Res. 2012;347: 141–54. pmid:22105921
    View Article   • PubMed/NCBI   • Google Scholar

12. Kaneto H, Morrissey J, Klahr S. Increased expression of TGF-beta 1 mRNA in the obstructed kidney of rats with unilateral ureteral ligation. Kidney Int. 1993;44: 313–21. Available: http://www.ncbi.nlm.nih.gov/pubmed/8377375 pmid:8377375
    View Article   • PubMed/NCBI   • Google Scholar

13. Sharma AK, Mauer SM, Kim Y, Michael AF. Interstitial fibrosis in obstructive nephropathy. Kidney Int. 1993;44: 774–88. Available: http://www.ncbi.nlm.nih.gov/pubmed/8258955 pmid:8258955
    View Article   • PubMed/NCBI   • Google Scholar

14. Nguyen G, Delarue F, Burcklé C, Bouzhir L, Giller T, Sraer J-D. Pivotal role of the renin/prorenin receptor in angiotensin II production and cellular responses to renin. J Clin Invest. 2002;109: 1417–1427. pmid:12045255
    View Article   • PubMed/NCBI   • Google Scholar

15. Huang Y, Wongamorntham S, Kasting J, McQuillan D, Owens RT, Yu L, et al. Renin increases mesangial cell transforming growth factor-beta1 and matrix proteins through receptor-mediated, angiotensin II-independent mechanisms. Kidney Int. 2006;69: 105–13. pmid:16374430

View Article   • PubMed/NCBI   • Google Scholar

16. Sakoda M, Ichihara A, Kaneshiro Y, Takemitsu T, Nakazato Y, Nabi AHMN, et al. (Pro)renin receptor-mediated activation of mitogen-activated protein kinases in human vascular smooth muscle cells. Hypertens Res. 2007;30: 1139–46. pmid:18250563
View Article   • PubMed/NCBI   • Google Scholar

17. Krishnamurthy P, Rajasingh J, Lambers E, Qin G, Losordo DW, Kishore R. IL-10 inhibits inflammation and attenuates left ventricular remodeling after myocardial infarction via activation of STAT3 and suppression of HuR. Circ Res. 2009;104: e9–18. pmid:19096025
View Article   • PubMed/NCBI   • Google Scholar

18. Krishnamurthy P, Lambers E, Verma S, Thorne T, Qin G, Losordo DW, et al. Myocardial knockdown of mRNA-stabilizing protein HuR attenuates post-MI inflammatory response and left ventricular dysfunction in IL-10-null mice. FASEB J. 2010;24: 2484–94. pmid:20219984
View Article   • PubMed/NCBI   • Google Scholar

19. Rajasingh J, Bord E, Luedemann C, Asai J, Hamada H, Thorne T, et al. IL-10-induced TNF-alpha mRNA destabilization is mediated via IL-10 suppression of p38 MAP kinase activation and inhibition of HuR expression. FASEB J. 2006;20: 2112–4. pmid:16935932
View Article   • PubMed/NCBI   • Google Scholar

20. Morrissey JJ, Klahr S. Effect of AT2 receptor blockade on the pathogenesis of renal fibrosis. Am J Physiol. 1999;276: F39–45. Available: http://www.ncbi.nlm.nih.gov/pubmed/9887078 pmid:9887078
View Article   • PubMed/NCBI   • Google Scholar

21. Morrissey JJ, Klahr S. Rapid communication. Enalapril decreases nuclear factor kappa B activation in the kidney with ureteral obstruction. Kidney Int. 1997;52: 926–33. Available: http://www.ncbi.nlm.nih.gov/pubmed/9328931 pmid:9328931
View Article   • PubMed/NCBI   • Google Scholar

22. Morrissey JJ, Ishidoya S, McCracken R, Klahr S. The effect of ACE inhibitors on the expression of matrix genes and the role of p53 and p21 (WAF1) in experimental renal fibrosis. Kidney Int Suppl. 1996;54: S83–7. Available: http://www.ncbi.nlm.nih.gov/pubmed/8731201 pmid:8731201
View Article   • PubMed/NCBI   • Google Scholar

23. Ishidoya S, Morrissey J, McCracken R, Klahr S. Delayed treatment with enalapril halts tubulointerstitial fibrosis in rats with obstructive nephropathy. Kidney Int. 1996;49: 1110–9. Available: http://www.ncbi.nlm.nih.gov/pubmed/8691732 pmid:8691732
View Article   • PubMed/NCBI   • Google Scholar

24. Ishidoya S, Morrissey J, McCracken R, Reyes A, Klahr S. Angiotensin II receptor antagonist ameliorates renal tubulointerstitial fibrosis caused by unilateral ureteral obstruction. Kidney Int. 1995;47: 1285–94. Available: http://www.ncbi.nlm.nih.gov/pubmed/7637258 pmid:7637258
View Article   • PubMed/NCBI   • Google Scholar

25. Brenner BM, Cooper ME, de Zeeuw D, Keane WF, Mitch WE, Parving HH, et al. Effects of losartan on renal and cardiovascular outcomes in patients with type 2 diabetes and nephropathy. N Engl J Med. 2001;345: 861–9. pmid:11565518
View Article   • PubMed/NCBI   • Google Scholar

26. Hou FF, Zhang X, Zhang GH, Xie D, Chen PY, Zhang WR, et al. Efficacy and safety of benazepril for advanced chronic renal insufficiency. N Engl J Med. 2006;354: 131–40. pmid:16407508
View Article   • PubMed/NCBI   • Google Scholar

27. Müller DN, Luft FC. Direct renin inhibition with aliskiren in hypertension and target organ damage. Clin J Am Soc Nephrol. 2006;1: 221–8. pmid:17699210
View Article   • PubMed/NCBI   • Google Scholar

28. Dominici M, Le Blanc K, Mueller I, Slaper-Cortenbach I, Marini F, Krause D, et al. Minimal criteria for defining multipotent mesenchymal stromal cells. The International Society for Cellular Therapy position statement. Cytotherapy. 2006;8: 315–7. pmid:16923606
View Article   • PubMed/NCBI   • Google Scholar

29. Minguell JJ, Erices A, Conget P. Mesenchymal stem cells. Exp Biol Med (Maywood). 2001;226: 507–20. Available: http://www.ncbi.nlm.nih.gov/pubmed/11395921
View Article   • Google Scholar

30. Yi T, Song SU. Immunomodulatory properties of mesenchymal stem cells and their therapeutic applications. Arch Pharm Res. 2012;35: 213–21. pmid:22370776
View Article   • PubMed/NCBI   • Google Scholar

31. Reinders MEJ, Roemeling-van Rhijn M, Khairoun M, Lievers E, de Vries DK, Schaapherder AFM, et al. Bone marrow-derived mesenchymal stromal cells from patients with end-stage renal disease are suitable for autologous therapy. Cytotherapy. 2013;15: 663–72. pmid:23419679
View Article   • PubMed/NCBI   • Google Scholar

32. Reinders MEJ, Fibbe WE, Rabelink TJ. Multipotent mesenchymal stromal cell therapy in renal disease and kidney transplantation. Nephrol Dial Transplant. 2010;25: 17–24. pmid:19861311
View Article   • PubMed/NCBI   • Google Scholar

33. Doorn J, Moll G, Le Blanc K, van Blitterswijk C, de Boer J. Therapeutic applications of mesenchymal stromal cells: paracrine effects and potential improvements. Tissue Eng Part B Rev. 2012;18: 101–15. pmid:21995703
View Article   • PubMed/NCBI   • Google Scholar

34. Cantaluppi V, Biancone L, Quercia A, Deregibus MC, Segoloni G, Camussi G. Rationale of mesenchymal stem cell therapy in kidney injury. Am J Kidney Dis. 2013;61: 300–9. pmid:22938846
View Article   • PubMed/NCBI   • Google Scholar

35. Wang S, Qu X, Zhao RC. Clinical applications of mesenchymal stem cells. J Hematol Oncol. 2012;5: 19. pmid:22546280
View Article   • PubMed/NCBI   • Google Scholar

36. Gregorini M, Bosio F, Rocca C, Corradetti V, Valsania T, Pattonieri EF, et al. Mesenchymal stromal cells reset the scatter factor system and cytokine network in experimental kidney transplantation. BMC Immunol. 2014;15: 44. pmid:25277788
View Article   • PubMed/NCBI   • Google Scholar

37. Rampino T, Gregorini M, Bedino G, Piotti G, Gabanti E, Ibatici A, et al. Mesenchymal stromal cells improve renal injury in anti-Thy 1 nephritis by modulating inflammatory cytokines and scatter factors. Clin Sci (Lond). 2011;120: 25–36.
View Article   • Google Scholar

38. Gregorini M, Maccario R, Avanzini MA, Corradetti V, Moretta A, Libetta C, et al. Antineutrophil cytoplasmic antibody-associated renal vasculitis treated with autologous mesenchymal stromal cells: evaluation of the contribution of immune-mediated mechanisms. Mayo Clin Proc. 2013;88: 1174–9. pmid:24079687
View Article   • PubMed/NCBI   • Google Scholar

39. Ciccocioppo R, Camarca A, Cangemi GC, Radano G, Vitale S, Betti E, et al. Tolerogenic effect of mesenchymal stromal cells on gliadin-specific T lymphocytes in celiac disease. Cytotherapy. 2014;16: 1080–91. pmid:24831843
View Article   • PubMed/NCBI   • Google Scholar

40. Ciccocioppo R, Bernardo ME, Sgarella A, Maccario R, Avanzini MA, Ubezio C, et al. Autologous bone marrow-derived mesenchymal stromal cells in the treatment of fistulising Crohn's disease. Gut. 2011;60: 788–98. pmid:21257987
View Article   • PubMed/NCBI   • Google Scholar

41. Semedo P, Correa-Costa M, Antonio Cenedeze M, Maria Avancini Costa Malheiros D, Antonia dos Reis M, Shimizu MH, et al. Mesenchymal stem cells attenuate renal fibrosis through immune modulation and remodeling properties in a rat remnant kidney model. Stem Cells. 2009;27: 3063–73. pmid:19750536
View Article   • PubMed/NCBI   • Google Scholar

42. Asanuma H, Vanderbrink BA, Campbell MT, Hile KL, Zhang H, Meldrum DR, et al. Arterially delivered mesenchymal stem cells prevent obstruction-induced renal fibrosis. J Surg Res. 2011;168: e51–9. pmid:20850784
View Article   • PubMed/NCBI   • Google Scholar

43. Liu X, Shen W, Yang Y, Liu G. Therapeutic implications of mesenchymal stem cells transfected with hepatocyte growth factor transplanted in rat kidney with unilateral ureteral obstruction. J Pediatr Surg. 2011;46: 537–45. pmid:21376206
View Article   • PubMed/NCBI   • Google Scholar

44. Ueno T, Nakashima A, Doi S, Kawamoto T, Honda K, Yokoyama Y, et al. Mesenchymal stem cells ameliorate experimental peritoneal fibrosis by suppressing inflammation and inhibiting TGF-β1 signaling. Kidney Int. 2013;84: 297–307. pmid:23486522
View Article   • PubMed/NCBI   • Google Scholar

45. Okabe M, Ikawa M, Kominami K, Nakanishi T, Nishimune Y. "Green mice" as a source of ubiquitous green cells. FEBS Lett. 1997;407: 313–9. Available: http://www.ncbi.nlm.nih.gov/pubmed/9175875 pmid:9175875
View Article   • PubMed/NCBI   • Google Scholar

46. Rampino T, Gregorini M, Bosio F, Bedino G, Corradetti V, Rocca C, et al. [Mesenchymal stromal cells injection reduces acute rejection damage in a rat experimental model of kidney transplantation]. | L'infusione di cellule mesenchimali stromali riduce il danno del rigetto acuto in un modello sperimentale di trapianto di rene ne. G Ital Nefrol. 2011;28: 132–134. pmid:21488020
View Article   • PubMed/NCBI   • Google Scholar

47. Chaabane W, Praddaude F, Buleon M, Jaafar A, Vallet M, Rischmann P, et al. Renal functional decline and glomerulotubular injury are arrested but not restored by release of unilateral ureteral obstruction (UUO). Am J Physiol Renal Physiol. 2013;304: F432–9. pmid:23220725
View Article   • PubMed/NCBI   • Google Scholar

48. Zonta S, De Martino M, Bedino G, Piotti G, Rampino T, Gregorini M, et al. Which is the most suitable and effective route of administration for mesenchymal stem cell-based immunomodulation therapy in experimental kidney transplantation: endovenous or arterial? Transplant Proc. 2010;42: 1336–40. pmid:20534295
View Article   • PubMed/NCBI   • Google Scholar

49. De Martino M, Zonta S, Rampino T, Gregorini M, Frassoni F, Piotti G, et al. Mesenchymal stem cells infusion prevents acute cellular rejection in rat kidney transplantation. Transplant Proc. 2010;42: 1331–5. pmid:20534294
View Article   • PubMed/NCBI   • Google Scholar

50. Vernon MA, Mylonas KJ, Hughes J. Macrophages and renal fibrosis. Semin Nephrol. 2010;30: 302–17. pmid:20620674
View Article   • PubMed/NCBI   • Google Scholar

51. Duffield JS. Macrophages and immunologic inflammation of the kidney. Semin Nephrol. 2010;30: 234–54. pmid:20620669
View Article   • PubMed/NCBI   • Google Scholar

52. Ricardo SD, van Goor H, Eddy AA. Macrophage diversity in renal injury and repair. J Clin Invest. 2008;118: 3522–30. pmid:18982158
View Article   • PubMed/NCBI   • Google Scholar

53. Wang Y, Harris DCH. Macrophages in renal disease. J Am Soc Nephrol. 2011;22: 21–7. pmid:21209251
View Article   • PubMed/NCBI   • Google Scholar

54. Aggarwal S, Pittenger MF. Human mesenchymal stem cells modulate allogeneic immune cell responses. Blood. 2005;105: 1815–22. pmid:15494428
View Article   • PubMed/NCBI   • Google Scholar

55. Suzuki T, Iyoda M, Shibata T, Ohtaki H, Matsumoto K, Shindo-Hirai Y, et al. Therapeutic effects of human mesenchymal stem cells in Wistar-Kyoto rats with anti-glomerular basement membrane glomerulonephritis. PLoS One. 2013;8: e67475. pmid:23826305
View Article   • PubMed/NCBI   • Google Scholar

56. Greish S, Abogresha N, Abdel-Hady Z, Zakaria E, Ghaly M, Hefny M. Human umbilical cord mesenchymal stem cells as treatment of adjuvant rheumatoid arthritis in a rat model. World J Stem Cells. 2012;4: 101–9. pmid:23189211
View Article   • PubMed/NCBI   • Google Scholar

57. Iwai N, Inagami T, Ohmichi N, Kinoshita M. Renin is expressed in rat macrophage/monocyte cells. Hypertension. 1996;27: 399–403. Available: http://www.ncbi.nlm.nih.gov/pubmed/8698444 pmid:8698444
View Article   • PubMed/NCBI   • Google Scholar

58. Adams DJ, Beveridge DJ, van der Weyden L, Mangs H, Leedman PJ, Morris BJ. HADHB, HuR, and CP1 bind to the distal 3'-untranslated region of human renin mRNA and differentially modulate renin expression. J Biol Chem. 2003;278: 44894–903. pmid:12933794
View Article   • PubMed/NCBI   • Google Scholar

59. Morris BJ, Adams DJ, Beveridge DJ, van der Weyden L, Mangs H, Leedman PJ. cAMP controls human renin mRNA stability via specific RNA-binding proteins. Acta Physiol Scand. 2004;181: 369–73. pmid:15283747
View Article   • PubMed/NCBI   • Google Scholar

60. Ma X, Che N, Gu Z, Huang J, Wang D, Liang J, et al. Allogenic mesenchymal stem cell transplantation ameliorates nephritis in lupus mice via inhibition of B-cell activation. Cell Transplant. 2013;22: 2279–90. pmid:23127285
View Article   • PubMed/NCBI   • Google Scholar

61. Pati S, Gerber MH, Menge TD, Wataha KA, Zhao Y, Baumgartner JA, et al. Bone marrow derived mesenchymal stem cells inhibit inflammation and preserve vascular endothelial integrity in the lungs after hemorrhagic shock. PLoS One. 2011;6: e25171. pmid:21980392
View Article   • PubMed/NCBI   • Google Scholar

62. Visavadiya NP, Li Y, Wang S. High glucose upregulates upstream stimulatory factor 2 in human renal proximal tubular cells through angiotensin II-dependent activation of CREB. Nephron Exp Nephrol. 2011;117: e62–70. pmid:20814220
View Article   • PubMed/NCBI   • Google Scholar

63. Vidotti DB, Casarini DE, Cristovam PC, Leite CA, Schor N, Boim MA. High glucose concentration stimulates intracellular renin activity and angiotensin II generation in rat mesangial cells. Am J Physiol Renal Physiol. 2004;286: F1039–45. pmid:14722017
View Article   • PubMed/NCBI   • Google Scholar